Early chronic low-level lead exposure produces glomerular hypertrophy in young C57BL/6J mice[☆]

John M. Basgen[a,*] and **Christina Sobin**[b,c,d]

[a] Life Sciences Institute, Charles R. Drew University of Medicine and Science, 1731 E 120th Street, Los Angeles, CA 90059, USA

[b] Department of Public Health Sciences, College of Health Science, University of Texas, El Paso, El Paso, TX 79902, USA

[c] Border Biomedical Research Center, College of Science, University of Texas, El Paso, El Paso, TX, USA

[d] Laboratory of Neuroendocrinology, The Rockefeller University, New York, NY, USA

Abstract

Early chronic lead exposure continues to pose serious health risks for children, particularly those living in lower socioeconomic environments. This study examined effects on developing glomeruli in young C57BL/6J mice exposed to low (30 ppm), higher (330 ppm) or no lead via dams' drinking water from birth to sacrifice on post-natal day 28. Low-level lead exposed mice [BLL mean (SD); 3.19 (0.70) µg/dL] had an increase in glomerular volume but no change in podocyte number compared to control mice [0.03 (0.01) µg/dL]. Higher-level lead exposed mice [14.68 (2.74) µg/dL] had no change in either glomerular volume or podocyte number. The increase in glomerular volume was explained by increases in glomerular capillary and mesangial volumes with no change in podocyte volume. Early chronic lead exposure yielding very low blood lead levels alters glomerular development in pre-adolescent animals.

Keywords

Pb toxicity; Glomerular hypertrophy; Capillary volume; Mesangial volume; Design-based stereology

1. Introduction

Exposure to lead has affected humans for millennia. Despite a dramatic reduction of environmental lead in the United States over the past 40 years, high levels persist in many lower socioeconomic neighborhoods (Lanphear et al., 2002). Child research has helped to increase recognition that no level of lead exposure is safe for children, and clinical studies have repeatedly shown the ill-effects of developmental lead exposure on organ systems.

[*] Corresponding author. Tel.: +1 3233573668. johnbasgen@cdrewu.edu, basgen@umn.edu (J.M. Basgen).. casobin@utep.edu (C. Sobin)

The first report of an association between lead exposure and kidney disease was more than one hundred years ago and has been followed by many subsequent reports (de Burbure et al., 2006; Fels et al., 1998; Steenland et al., 1992). For many years, the link between lead exposure and kidney disease was controversial. While findings from some reports suggested a direct relationship between kidney disease and lead exposure (Ekong et al., 2006; Fadrowski et al., 2010), others suggested that preexisting kidney disease prevented adequate excretion of ingested or inhaled lead thus increasing blood and body lead burden and its deleterious effects (Staessen et al., 1990). Some of the controversy may have been due to the broad variability in lead exposure levels examined and age related differences in lead metabolism (Lidsky and Schneider, 2003). Lead absorption is greater and retention is longer in children as compared to adults (Ziegler et al., 1978). Also, exposure during early development may affect kidneys differently than exposure during late adolescence or adulthood. More recently, studies have confirmed the association between lead exposure and kidney damage (Spector et al., 2011), and a few have suggested adverse effects of very low-level lead exposure on developing kidney. Glomerular filtration rate (GFR) is a measure of kidney function and is used to diagnose kidney injury and failure. GFR is a well-established indicator of early-stage diabetic nephropathy, hypertensive nephropathy, and other renal diseases. For example, recent studies showed that GFR was elevated even in pre-diabetics and pre-hypertensive patients (Fadrowski et al., 2010; Okada et al., 2012). Progressive kidney disease has been shown to be characterized by a decrease to abnormally low GFR followed by eventual glomerulosclerosis (Palatini et al., 2012). Increased GFR is associated with glomerular hypertrophy in both diabetic patients and animal models of diabetes (Østerby and Gundersen, 1975; Seyer-Hansen et al., 1980). It has been hypothesized that stress within hypertrophic glomeruli initiates changes in the glomerulus resulting in glomerulosclerosis (Nagata et al., 1992).

Kidney development results from a complex interaction of diverse metabolic pathways that are dependent on transcription factors, cytokines, growth factors, angiotensin II, and other contributing processes (Cain et al., 2010; Carroll and Das, 2013). Kidney development occurs as the ureteric bud undergoes repeated branching, with each branch point meeting metanephric mesenchyme. This branching process produces four morphologically distinguishable stages of glomerular development including the comma-shaped body, s-shaped body, capillary loop stage, and mature glomerulus (Reeves et al., 1978). Disruption of development during any of these stages may produce maldeveloped kidneys, which may in turn result in low body weight, low glomerular number, and glomerular hypertrophy at birth; and notably, hypertension and kidney disease later in life (Keller et al., 2003; Schreuder, 2012). Early lead exposure may disrupt glomerular development which could manifest as hypertension and kidney disease later in life long after lead has cleared from the body. Such effects might partially explain high rates of idiopathic kidney disease that have observed in specific minority populations (Hsu et al., 2003) living in lower socioeconomic neighborhoods with increased likelihood of environmental lead exposure.

Animal studies have not yet examined effects on kidney structure of chronic low-level developmental lead exposure. In rodent kidney, where glomerulogenesis and glomerular development continue for several weeks after birth (Ciuffo et al., 1993), chronic post-partum exposure to lead could provide a model of low-level lead induced nephrotoxicity, including glomerular maldevelopment. The aim of these studies was to examine whether chronic exposure to lead in young C57BL/6J mice resulted in maldeveloped glomeruli. If so, the findings could suggest a model for studying possible links between early chronic exposure to lead and hypertension and kidney disease in adulthood.

2. Materials and methods

2.1. Animals

C57BL/6J (Jax Mice, Jackson Laboratory, Sacramento, CA) were bred and housed at the University of Texas at El Paso Biosciences Research Facility vivarium. Individual litters were kept in polycarbonate cages with wood chip bedding. The mice were maintained on a 12 h light–dark schedule at a temperature of 21 ± 2 °C with ad libitum access to food and water. The drinking water of the dams was treated with 99.4% lead acetate. No invasive procedures were conducted during the 28-day exposure time. Natural litters were exposed from birth to one of three lead doses: 0, 30, or 330 ppm, selected after pilot studies demonstrated that 30–40 ppm of lead acetate in dams' drinking water yielded a range of blood lead levels that overlapped those of approximately 60% of low-income children tested in our child lead exposure studies (unpublished data). Twelve mice per group (six male and six female) were used for analysis. This study was carried out following a protocol approved by the Animal Care and Use Committee of the University of Texas at El Paso (NIH Assurance #A3340-01) in accordance with the Guide for the Care and Use of Laboratory Animals of the National Institutes of Health.

2.2. Analysis of blood lead

Mice were anesthetized with Avertin at post-natal day 28 (PND 28). When full anesthesia was confirmed (via absence of blink response and paw-pinch reflexes) the chest cavity was opened and 50 µl of blood was drawn from the apex of the heart for inductively coupled plasma mass spectrometry (ICP-MS) analysis of blood lead level.

Analysis ICP-MS was performed with an Agilent 7500ce ICP/MS equipped with an octopole reaction system and a CETAC ASX-520 autosampler as previously described (Sobin et al., 2011a). Briefly, samples were introduced to the plasma through a MicroMist U-series nebulizer (Glass Expansion, Australia) and a double-pass quartz spray chamber (Agilent, Santa Clara, CA). Instrument parameters were: carrier gas, 0.78 L/min; makeup gas, 0.15 L/min; RF power, 1420 W; spray chamber temperature, 2 °C.

Certified whole blood standards (Le Center de Toxicologie du Quebec) were analyzed to determine instrument reproducibility and validate quantitation. Ten solutions were prepared for each of two standards (4.00 and 6.59 µg/dL) and each of those were analyzed three times by ICP-MS. Standard concentrations were chosen to approximate low blood Pb values of children in this study. Blood standards were prepared as previously described (Sobin et al., 2011b) (Agilent technical note #5988-0533EN). Briefly, 5.58 mL of water (18 MΩ DI, Labconco WaterPro® PS Station, Kansas City, MO) was placed in a polypropylene tube into which 300 µL of whole blood was added, followed by addition of 60 µL of aqueous internal standard solution (100 ppb each germanium, yttrium and terbium in 5% nitric acid, Fisher Optima) and 60 µL of aqueous 10 ppm gold in 3% hydrochloric acid (EMD Chemicals) solution. The final dilution was twenty-fold, the final internal standard concentration was 1 ppb and the final gold concentration was 100 ppb. A six-point external calibration curve was prepared from a Pb stock solution in 1% nitric acid. ICP-MS standard solutions containing the elements in 2% nitric acid were obtained from Inorganic Ventures (Christiansburg, VA). Samples were vortexed for a few seconds prior to a one minute centrifugation at 2000 rcf and the supernatant analyzed by ICP-MS. Blank solutions were analyzed after every three samples throughout the analytical sequence and standard check solutions were analyzed five times, interspersed through the sequence. All samples produced signals in excess of the limit of quantitation (i.e. ten-fold greater than the detection limit) for each analyte.

2.3. Tissue processing

Animals were perfused transcardially with 10% sucrose followed by phosphate-buffered 4% paraformaldehyde. Fixed kidneys were removed and stored in the same fixative at 4 °C for approximately 6 weeks. Kidneys were weighed and 1-mm cubes were cut from the cortex, washed three times in buffer, post-fixed in 1% osmium tetroxide for one hour, washed three times in buffer, and embedded in Polybed 812 (Polysciences, Inc., Warrington, PA). One female kidney from the low-dose group was not adequately perfuse-fixed and thus was not used for morphometric analysis. Tissue was examined via light and electron microscopy.

2.4. Podocyte number and glomerular volume via light microscopy: Study 1

Light microscopy methods were used to compare glomerular volume, podocyte number and podocyte numerical density in three groups (controls, 30 ppm and 330 ppm).

2.4.1. Sectioning—Serial 1-mm thick sections were cut from one or two tissue blocks per kidney using an EM UC7 ultramicrotome (Leica Microsystems, Buffalo Grove, IL) fitted with a Histo Jumbo diamond knife (Diatome US, Hatfield, PA). The first section from a block with no holes was saved to a glass slide and stained with 0.5% toluidine blue. This slide was labeled 0. Subsequently, every 10th section and the adjacent section were saved to a new slide, stained with toluidine blue and the slides labeled 10, 20, 30, etc. Twenty pairs of sections were saved from each kidney and used for light microscopy analysis.

2.4.2. Imaging—All imaging was conducted blind to experimental group and blind to mouse blood lead level. A BX51 microscope with DP 71 digital camera and DB Controller software (Olympus America, Inc., Cypress, CA) was used to obtain images. A map of all the glomeruli present in the section on slide 0 was drawn using the 10× objective lens. (Glomeruli on slide 0 were necessarily partial objects and were not used for morphometry). Next, the two sections on slide 10 were examined and compared to slide 0. All newly appearing glomeruli were identified, mapped, numbered sequentially and imaged using the 100× objective lens (NA = 1.40). These glomeruli and new glomeruli appearing on subsequent slides were imaged using the subsequent pairs of sections until each glomerulus disappeared. Ten glomeruli were imaged per mouse. A stage micrometer was imaged and used to validate magnification. Image files were transferred to an Apple iMac Computer and viewed on a 24 in. monitor using Photoshop software (Adobe Systems, Inc., San Jose, CA). A Photoshop window magnification of 67% was used when making measurements.

2.4.3. Podocyte number—The number of podocytes per glomerulus was counted using the fractionator/disector method (Bai and Basgen, 2011; Nyengaard, 1999). Podocyte nuclei were counted as a surrogate for the number of podocytes assuming one and only one nucleus per podocyte. Using the two images of a glomerulus from each pair of sections, the number of profiles from a podocyte nucleus seen in the first section (the sample section) but not in the adjacent section (the look-up section) was counted (Fig. 1). This was repeated until all pairs of images (levels) from a glomerulus were analyzed. Podocyte number was calculated using the equation:

$$N_{\text{podocyte}} = 10 \times \sum Q^-$$

where 10 was the reciprocal of the fraction (1/10) of the glomerulus sampled. $\sum Q^-$ is the sum over all the section pairs from a glomerulus of nuclear profiles from podocytes seen in the sample sections but not in the look-up sections. Ten glomeruli per kidney were analyzed and the average number of podocytes per glomerulus was calculated.

2.4.4. Glomerular volume—Glomerular volume was estimated using the Cavalieri Principle (Bai and Basgen, 2011; Nyengaard, 1999). The glomerulus was defined as the minimal string polygon surrounding the glomerular tuft (Fig. 2). The sample section image from each pair of images from a glomerulus was used to estimate glomerular volume. Using the Layers function of Photoshop, a grid of points was randomly superimposed over each sample section image and the number of grid points touching the glomerulus was counted (Fig. 2). Glomerular volume was calculated using the equation

$$V_{\text{glomerulus}} = 10 \times \sum P \times (d/\text{mag})^2 \mu\text{m}^3$$

where 10 is the distance between the sample sections in μm, $\sum P$ is the sum of grid points counted touching the glomerulus in all sample sections images from the glomerulus, d is the distance between the points on the grid in μm, and mag is the magnification of the images. Volume was measured using 10 glomeruli from each kidney and the average glomerular volume for a mouse calculated.

2.4.5. Podocyte numerical density—The numerical density of podocyte per glomerular volume was calculated by dividing the number of podocytes counted in a glomerulus by the glomerular volume.

2.5. Volume of glomerular components via electron microscopy: Study 2

Differences between controls and low-dose mice in glomerular volume found in Study 1 necessitated further detailed analysis and comparison of glomerular components of controls and low-dose animals via electron microscopy.

2.5.1. Sectioning—For electron microscopy analysis, a single 1-μm thick section from each of several tissue blocks was saved and stained with toluidine blue. Using these scout sections, whole glomerular profiles at least one large glomerular diameter from the edge of the block were selected for thin sectioning. Using the same ultramicrotome fitted with an Ultra diamond knife (Diatome US), silver–gold sections were cut, placed on formvar-coated single slot grids and stained with uranyl acetate and lead citrate.

2.5.2. Imaging—All imaging was conducted blind to experimental group and blind to mouse blood lead level. A JEM1200-EX electron microscope (JEOL USA, Inc., Peabody, MA) fitted with a digital camera and DigitalMicrographs software (Gatan, Inc., Pleasanton, CA) was used to obtain EM images of complete glomerular profiles at an initial magnification of 3000×. For larger glomerular profiles, two to four images were needed to cover the entire profile. Image files were transferred to an Apple iMac Computer and viewed on a 24 in. monitor (Apple, Inc., Cupertino, CA) using Photoshop software (Adobe Systems, Inc.) and a window magnification of 100% was used for all measurements.

2.5.3. Volume density of glomerular components—The volume densities of glomerular components were estimated using the Delesse Principle (Weibel, 1979) on the EM images. The glomerulus was divided into four components: podocyte, mesangium, capillary lumen (including endothelial and circulating cells), and remainder components including Bowman's space, glomerular basement membrane, and non-resolvable tissue (Fig. 3A). The glomerulus was again defined as the minimal string polygon surrounding the glomerular tuft (Fig. 3B). A counting grid was randomly superimposed over the glomerular image; the number of grid points touching each of the four components was counted (Fig. 3B). The volume density of a component per glomerulus was calculated using the equation:

$$V_v \left(\text{Component} X / \text{glomerulus} \right) = P_{\text{Component} X} / \sum P_{\text{four components}}$$

where *X* represents a component, either podocyte, mesangium, capillary lumen, or remainder and $\sum P_{\text{four components}}$ is the sum of the points touching all four components. Ten glomerular profiles were measured per kidney and used to calculate the kidney mean for each component.

2.5.4. Volume of glomerular components—The volume of each individual glomerular component was calculated by multiplying the component volume density by the mean glomerular volume. For example, to calculate the volume of mesangium within a glomerulus:

$$\text{Volume}_{\text{mesangium}} = V_v \left(\text{Mesangium} / \text{glomerulus} \right) \times \text{Glomerular volume}, \quad \mu\text{m}^3$$

The volume of each glomerular component was calculated using each respective volume density.

2.6. Statistical analysis

SAS Version 9.2 statistical software was used for all analyses. Entered data were checked for accuracy and distribution properties; no outliers were identified and all data were included for analysis. For Study 1, blood lead level, body weight and kidney weight; and glomerular volume, podocyte volume density and podocyte number were compared using a 3 (group) $\times$ 2 (sex) general linear model ANOVA, which also indicated amount of variance explained (R^2) for each model. For Study 2, podocyte, mesangium, capillary lumen (including endothelial and circulating cells), and remainder component volume differences were compared using a 2 (group) $\times$ 2 (sex) general linear model ANOVA. Type III sum of squares was used to determine statistically significant differences ($p < .05$); post hoc tests of marginal means ("least square means") were conducted for all significant models. (Least square means are the means of each subgroup corrected for all other factors in the model.)

3. Results

3.1. Clinical characteristics

Table 1 shows the means and standard deviations for blood lead level, body weight and kidney weight, by exposure group and sex at sacrifice (PND 28). Lead treatments yielded the expected group differences in blood lead level as determined by ICP-MS ($F = 134.91$, $p < .01$; $R^2 = 0.96$). Differences were accounted for by independent effects of group (Type III SS, $F = 331.77$, $p < .01$) and sex (Type III SS, $F = 5.85$, $p = .02$). Within treated groups, blood lead levels were higher in males. The group $\times$ sex interaction was not significant.

Body weight at sacrifice differed ($F = 4.21$, $p < .01$; $R^2 = 0.41$), accounted for by independent effects of group (Type III SS, $F = 3.64$, $p = .04$) and sex (Type III SS, $F = 13.0$, $p < .01$); the group $\times$ sex interaction was not significant. Least square means for body weight of low-dose (12.89 g) and high-dose (12.92 g) animals did not differ; the body weight for both experimental groups was less than that of controls (14.12 g) ($p = .03$ for both comparisons). Also, females (12.54 g) weighed less than males (14.08 g) ($p < .01$). The interaction of group $\times$ sex was not significant.

Kidney weight also differed ($F = 3.27$, $p = .02$; $R^2 = 0.37$), again accounted for by independent effects of group (Type III SS, $F = 3.60$, $p = .04$) and sex (Type III SS, $F = 7.21$, $p = .01$) with no interaction effect. Post hoc tests of least squared means revealed that group differences in kidney weight were accounted for by reduced kidney weight among only the low-dose animals (0.09 g) ($p = 01$) (Table 1). Kidney weights of control (0.10 g) and high-dose (0.10 g) animals did not differ.

3.2. Podocyte number and glomerular volume: Study 1 (light microscopy)

Table 2 shows the means and standard deviations for podocyte number, glomerular volume, and podocyte numerical density.

3.2.1. Podocyte number—The mean number of podocyte Q^-s counted per mouse was 136 (range: 102–169). Podocyte number did not differ among groups.

3.2.2. Glomerular volume (μm^3)—The mean number of profiles (levels) measured per glomerulus was 5.4 (range: 3–8) with a mean of 374 (range: 313–479) grid points counted per mouse. Glomerular volume differed among groups ($F = 5.20$, $p < .01$; $R^2 = 0.47$) and differences were accounted for by exposure group (Type III SS, $F = 12.58$, $p < .01$). Post hoc tests of least square means showed that glomerular volume of low-dose animals (86,898 μm^3) was greater than that of controls (72,215 μm^3) ($p < .01$) and high dose animals (77,328 μm^3) ($p < .01$) (Fig. 4).

3.2.3. Podocyte numerical density—Podocyte volume density did not differ among groups. It was noted that the R^2 for this model was 0.24, and the Type III SS for the group effect was significant ($F = 3.77$, $p = .03$), however the model F was not significant ($F = 1.86$, $p = .13$). (Glomerular density tended to be reduced only among low-dose animals.)

3.3. Volume of glomerular components: Study 2 (electron microscopy)

To examine the possible sources of increased glomerular volume in low-dose lead exposed animals, densities and volumes of podocytes, capillary lumen (including endothelial and circulating cells); mesangium; and remainder components (including Bowman's space, glomerular basement membrane, and non-resolvable tissue) were estimated for low-dose lead exposed and control animals using electron microscopy. Table 3 shows the means and standard deviations for each of these components by group and sex.

3.3.1. Glomerular component volume densities—The mean number of grid points counted per animal was 632 (range: 324–961). Control and lead-exposed animals did not differ with regard to volume density of podocytes; capillary lumen; mesangium; and remainder components (Table 3).

3.3.2. Glomerular component volumes

3.3.2.1. Podocyte volume: Podocyte volume did not differ between groups. It was noted however that while the model F did not reach significance ($F = 2.39$, $p = .10$) the Type III SS for the main effect group ($F = 6.82$, $p = .02$) was significant ($R^2 = 0.27$). The broad variability of podocyte volume values among the exposed group showed that a larger sample size might be needed to statistically detect differences in podocyte volume (Fig. 5A).

3.3.2.2. Mesangial volume: Mesangial volume differed between groups ($F = 5.12$, $p < .01$; $R^2 = 0.45$) accounted for by independent effects of exposure group (Type III SS $F = 10.97$, $p < .01$) and sex ($F = 4.85$, $p < .05$). Mesangial volume was larger in low-dose animals (LS mean = 16,825, SE = 829) as compared with controls (13,027, SE = 791). Also, regardless

of exposure, mesangial volume in females (LS mean = 16,189, SE = 830) was greater than in males (LS mean = 13,663, SE = 791) (Fig. 5B). The interaction of exposure × sex was not significant.

3.3.2.3. Capillary volume: Capillary lumen volume, including endothelial and circulating cells, differed between groups ($F = 8.46$, $p < .01$; $R^2 = 0.57$) accounted for by only exposure (Type III SS $F = 15.05$, $p < .01$). Capillary lumen volume was larger in low-dose animals (LS mean = 33,671; SE = 984) as compared with controls (LS mean = 27,216; SE = 939) (Fig. 5C).

3.3.2.4. Remainder component volume: The "remainder component" did not differ between groups ($F = 0.99$, $p = .42$; $R^2 = 0.14$).

4. Discussion

Hundreds of child and adult studies have examined the effects of lead exposure on organs and bodily systems. Very few studies however examined effects associated with chronic low-level exposure yielding very low blood lead levels. One such study showed that among 769 children and adolescents with blood lead levels between 1.6 and 4.1 µg/dL, cystatin-C estimated glomerular filtration rate was inversely associated with blood lead level (Fadrowski et al., 2010) suggesting a dose response relationship even at lowest levels of exposure. These findings may have profound implications for the health and development of large numbers of low-income children. In our studies of 648 school children between the ages of 5 and 12 years and living in lower socioeconomic conditions, approximately 70% had blood lead levels of 1.6 µg/dL or higher (unpublished data). Other clinical studies have suggested that large numbers of low-income children in particular have blood lead levels greater than 1.6 µg/dL suggesting the need to understand the effects on kidney development of low level lead exposure yielding low blood lead levels.

In the animal literature, only six studies thus far have examined effects of early chronic lead exposure yielding low blood lead levels that overlap those of high-risk children (Azzaoui et al., 2009; Ferguson and Bowman, 1990; Kasten-Jolly et al., 2012; Leasure et al., 2008; Reiter et al., 1975; Sobin et al., 2013); only one of those studied effects of low-level lead in young animals (Sobin et al., 2013). In the current studies, using light microscopy and unbiased stereological methods, we found that pre-adolescent lead exposed mice with blood lead levels between 2.4 and 4.7 µg/dL had increased glomerular volume as compared with controls and high dose animals (with blood lead levels between 11.7 and 20.3 µg/dL). Using electron microscopy and unbiased stereological methods, we found that increased glomerular volume was attributable to increased mesangial volume and increased capillary volume, but not increased podocyte volume ("remainder component" volumes also did not differ).

Growth hormones, notably, VEGF and TGF-β play an integral role in the normal development of the glomerulus (de Vriese et al., 2001; Liu et al., 1999), and specifically in the development of glomerular capillaries. Increased growth factors within the glomerulus have been shown to increase volume of the glomerulus, mesangium, and capillaries (de Vriese et al., 2001; Flyvbjerg et al., 2002); and growth hormone levels are increased in diabetic nephropathy. Increased growth hormone levels in animal models of kidney disease resulted in abnormal glomerular capillary and mesangial growth (Flyvbjerg et al., 2002).

Specifically with regard to lead exposure, Hossain et al. used microarray analysis to identify lead-sensitive genes in fetal human astrocytes. In lead exposed animals the growth hormone VEGF was one of the most highly expressed genes examined (Hossain et al., 2000). In

follow-up studies neonatal rats exposed to lead had a two-fold increase of VEGF expression in cerebellum as well as microvascular hemorrhage and increased vascular permeability to serum albumin (Hossain et al., 2004). In another set of studies Zuscik and colleagues showed that lead exposure enhanced the effect of TGF-β on chondrogenesis in murine limb bud mesenchymal cells (Zuscik et al., 2007).

With regard to the current findings, further studies are needed to examine whether increased capillary and mesangial growth in the low-dose animals induced overproduction of VEGF and TGF-β resulting in new glomerular capillary formation and mesangial expansion. Also, whether the structural changes observed in pre-adolescent mice predispose animals to perhaps abnormal GFR followed in adulthood by glomerulosclerosis needs to be examined.

In the current studies, structural changes to the glomerulus were unique to animals with blood lead levels between 2.4 and 4.7 µg/dL; no changes to the glomerulus were observed in animals with blood lead levels between 11.7 and 20.3 µg/dL. Replication and extension of these studies may eventually help to reveal why or how low level but not higher level lead exposure causes structural hypertrophic changes in the developing kidney. Additional studies are needed to examine, for example, whether blood lead levels above 10 µg/dL trigger protective mechanisms that assist in sequestering lead in bone, thereby rendering the absorbed lead unable to alter growth hormone levels. Complementary studies could examine whether lead sequestration is less likely in cases of low-level exposure, resulting in higher levels of circulating lead that are perhaps sufficient to stimulate overproduction of growth hormones and thus resulting in glomerular hypertrophy, abnormal GFR, and perhaps kidney disease in adulthood.

Podocytes play an important role in regulating the filtration of molecules through the glomerular filtration surface. Distortion in the architecture of the podocytes and later loss of podocytes is associated with the leakage of some proteins into the urine, another marker of kidney disease progression (Greka and Mundel, 2012). In this study of pre-adolescent animals, podocyte number and volume did not differ among groups. It is possible that the etiologic effects of hyperfiltration and deceased GFR on the health of podocytes is of relatively long duration, thus changes in podocyte number and volume might not be measurable until adulthood. Additional studies are needed to examine this possibility.

In addition to the structural differences observed, only the low-dose animals had significantly reduced kidney weight (both lead exposed groups had reduced body weight as compared with controls). If replicated this finding may provide an additional unique marker of low-level lead induced kidney pathology. Additional studies are needed to determine whether reduced kidney weight in the low-dose animals reflects an early stage of a disease process that diminishes normal tissue density.

Our findings of structural hypertrophic changes in low level lead exposed animals may be broadly consistent with changes that occur in the early stages of kidney disease. An increase in glomerular volume is an early marker of some kidney diseases (Hattori et al., 1993) and has been simulated in murine models of kidney disease (Suzuki et al., 2005). Glomerular hypertrophy results from increased glomerular capillary volume and surface area, and also increased mesangial volume (Hirose et al., 1980; Peppa et al., 2006). Nyengaard and Rasch (1993) have shown that such increases in the diabetic rat are the result of an increase in the number of capillaries within the glomerulus, which in turn increases the glomerular filtration surface and thus hypertrophy. These findings require replication. It will also be important to conduct long-term follow-up studies to determine whether in utero lead exposure decreases the number of glomeruli which may in turn predict hypertension and glomerular sclerosis in

later adulthood (following those developmental changes that may have had few clinical sequelae early in life).

More generally speaking, this study attempted to increase the relevance of findings to the problem of child low-level lead exposure in several ways. The exposure protocol was developed to yield a relatively narrow range of blood lead levels in the low-level exposure group that overlapped approximately 60% of the low-income children studied. Moreover, children in clinical low-level lead studies have typically been of pre-adolescent age thus in these studies animals were exposed from birth to PND 28, which is immediately prior to the onset of puberty. ICP-MS analysis of blood samples taken at sacrifice were used to confirm that our lead treatments (30 ppm and 330 ppm) produced a low-dose group with blood lead levels that overlapped those of a majority of our low-income child study participants, and a positive control group with significantly higher blood lead levels. Kidneys were harvested immediately upon sacrifice, sectioned and analyzed via light and electron microscopy and all studies were conducted blind to group and blood lead level. The hallmark of progressive kidney disease is a decrease in GFR while the early stages of some nephropathies include temporary increases in GFR, that is, hyperfiltration (Jerums et al., 2010). In this study, kidney function was not directly assessed; this limitation is being addressed in ongoing studies. These studies using unbiased designed-based stereological methods detected for the first time early glomerular structural changes in pre-adolescent mice that may predict progression to kidney failure in adulthood.

5. Conclusions

Structural markers of kidney maldevelopment including glomerular hypertrophy, capillary volume increase and mesangial expansion, and reduced kidney weight, are evident in a mouse model examining the effects on pre-adolescent kidney of chronic developmental low-level lead exposure yielding blood lead levels between 2.4 and 4.7 µg/dL. The findings raise important questions regarding the mechanisms that might explain effects at lowest but not higher levels of lead exposure. Additional studies are needed to examine the mechanistic relationships between lead exposure and these early structural changes and to examine whether these early changes are in fact markers of later kidney disease. Studies of the associations between structural and functional markers of disease are also needed. Given the large numbers of low-income minority children at high risk of chronic developmental low-level lead exposure, these findings may suggest early clues regarding one possible source of kidney disease in minority populations.

Acknowledgments

References

Azzaoui FZ, Ahami AO, Khadmaoui A. Impact of lead sub-chronic toxicity on recognition memory and motor activity of Wistar rat. Pak. J. Biol. Sci. 2009; 12:173–177. [PubMed: 19579940]

Bai XY, Basgen JM. Podocyte number in the maturing rat kidney. Am. J. Nephrol. 2011; 33:91–96. [PubMed: 21196721]

Cain JE, Di Giovanni V, Smeeton J, Rosenblum ND. Genetics of renal hypoplasia: insights into the mechanisms controlling nephron endowment. Pediatr. Res. 2010; 68:91–98. [PubMed: 20421843]

Carroll T, Das A. Defining the signals that constitute the nephron progenitor niche. Am. J. Kidney Dis. 2013; 24:873–876.

Ciuffo GM, Viswanathan M, Seltzer AM, Tsutsumi K, Saavedra JM. Glomerular angiotensin II receptor subtypes during development of rat kidney. Am. J. Physiol. 1993; 265:F264–F271. [PubMed: 8368335]

de Burbure C, Buchet JP, Leroyer A, Nisse C, Haguenoer JM, Mutti A, Smerhovsky Z, Cikrt M, Trzcinka-Ochocka M, Razniewska G, Jakubowski M, Bernard A. Renal and neurologic effects of cadmium, lead, mercury, and arsenic in children: evidence of early effects and multiple interactions at environmental exposure levels. Environ. Health Perspect. 2006; 114:584–590. [PubMed: 16581550]

de Vriese AS, Tilton RG, Elger M, Stephan CC, Kriz W, Lameire NH. Antibodies against vascular endothelial growth factor improve early renal dys-function in experimental diabetes. J. Am. Soc. Nephrol. 2001; 12:993–1000. [PubMed: 11316858]

Ekong EB, Jaar BG, Weaver VM. Lead-related nephrotoxicity: a review of the epidemiologic evidence. Kidney Int. 2006; 70:2074–2084. [PubMed: 17063179]

Fadrowski JJ, Navas-Acien A, Tellez-Plaza M, Guallar E, Weaver VM, Furth SL. Blood lead level and kidney function in us adolescents: the third national health and nutrition examination survey. Arch. Intern. Med. 2010; 170:75–82. [PubMed: 20065202]

Fels L, Wunsch M, Baranowski J, Norska-Borowka I, Price R, Taylor S, Patel S, De Broe M, Elsevier M, Lauwerys R, Roels H, Bernard A, Mutti A, Gelpi E, Rosello J, Stolte H. Adverse effects of chronic low level lead exposure on kidney function-a risk group study in children. Nephrol. Dial. Transpl. 1998; 13:2248–2256.

Ferguson SA, Bowman RE. Effects of postnatal lead exposure on open field behavior in monkeys. Neurotoxicol. Teratol. 1990; 12:91–97. [PubMed: 2333073]

Flyvbjerg AD-HF, DeVriese AS, Schrijvers BF, Tilton RG, Rasch R. Amelioration of long-term renal changes in obese type 2 diabetic mice by a neutralizing vascular endothelial growth factor antibody. Diabetes. 2002; 51:3090–3094. [PubMed: 12351452]

Greka A, Mundel P. Cell biology and pathology of podocytes. Annu. Rev. Physiol. 2012; 74:299–323. http://dx.doi.org/10.1146/annurev-physiol-020911-153238. [PubMed: 22054238]

Hattori M, Kim Y, Steffes MW, Mauer SM. Structural-functional relationships in type I mesangiocapillary glomerulonephritis. Kidney Int. 1993; 43:381–386. [PubMed: 8441233]

Hirose K, Tsuchida H, Osterby R, Gundersen HJ. A strong correlation between glomerular filtration rate and filtration surface in diabetic kidney hyperfunction. Lab. Invest. 1980; 43:434–437. [PubMed: 7421124]

Hossain MA, Bouton CM, Pevsner J, Laterra J. Induction of vascular endothelial growth factor in human astrocytes by lead Involvement of a protein kinase C/activator protein-1 complex-dependent and hypoxia-inducible factor 1-independent signaling pathway. J. Biol. Chem. 2000; 275:27874–27882. [PubMed: 10882716]

Hossain MA, Russell JC, Miknyoczki S, Ruggeri B, Lal B, Laterra J. Vascular endothelial growth factor mediates vasogenic edema in acute lead encephalopathy. Ann. Neurol. 2004; 55:660–667. [PubMed: 15122706]

Hsu CY, Lin F, Vittinghoff E, Shlipak MG. Racial differences in the progression from chronic renal insufficiency to end-stage renal disease in the United States. J. Am. Soc. Nephrol. 2003; 14:2902–2907. [PubMed: 14569100]

Jerums G, Premaratne E, Panagiotopoulos S, MacIsaac RJ. The clinical significance of hyperfiltration in diabetes. Diabetologia. 2010; 53:2093–2104. http://dx.doi.org/10.1007/s00125-010-1794-9. [PubMed: 20496053]

Kasten-Jolly J, Pabello N, Bolivar VJ, Lawrence DA. Developmental lead effects on behavior and brain gene expression in male and female BALB/cAnNTac mice. Neurotoxicology. 2012; 33:1005–1020. http://dx.doi.org/ 10.1016/j.neuro.2012.04.017. [PubMed: 22609695]

Keller G, Zimmer G, Mall G, Ritz E, Amann K. Nephron number in patients with primary hypertension. N. Engl. J. Med. 2003; 348:101–108. [PubMed: 12519920]

Lanphear BP, Hornung R, Ho M, Howard CR, Eberly S, Knauf K. Environmental lead exposure during early childhood. J. Pediatr. 2002; 140:40–47. [PubMed: 11815762]

Leasure JL, Giddabasappa A, Chaney S, Johnson JE, Pothakos K, Lau YS, Fox DA. Low-level human equivalent gestational lead exposure produces sexspecific motor and coordination abnormalities and late-onset obesity in year-old mice. Environ. Health Perspect. 2008; 116:355–361. [PubMed: 18335103]

Lidsky TI, Schneider JS. Lead neurotoxicity in children: basic mechanisms and clinical correlates. Brain. 2003; 126:5–19. [PubMed: 12477693]

Liu A, Dardik A, Ballermann BJ. Neutralizing TGF-beta1 antibody infusion in neonatal rat delays in vivo glomerular capillary formation 1. Kidney Int. 1999; 56:1334–1348. [PubMed: 10504486]

Nagata M, Scharer K, Kriz W. Glomerular damage after uninephrectomy in young rats I. Hypertrophy and distortion of capillary architecture. Kidney Int. 1992; 42:136–147. [PubMed: 1635343]

Nyengaard JR. Stereologic methods and their application in kidney research. J. Am. Soc. Nephrol. 1999; 10:1100–1123. [PubMed: 10232698]

Nyengaard JR, Rasch R. The impact of experimental diabetes mellitus in rats on glomerular capillary number and sizes. Diabetologia. 1993; 36:189–194. [PubMed: 8462766]

Okada R, Yasuda Y, Tsushita K, Wakai K, Hamajima N, Matsuo S. Glomerular hyperfiltration in prediabetes and prehypertension. Nephrol. Dial. Transpl. 2012; 27:1821–1825. http://dx.doi.org/10.1093/ndt/gfr651.

Østerby R, Gundersen HJ. Glomerular size and structure in diabetes mellitus. I. Early abnormalities. Diabetologia. 1975; 11:225–229. [PubMed: 1149955]

Palatini P, Dorigatti F, Saladini F, Benetti E, Mos L, Mazzer A, Zanata G, Garavelli G, Casiglia E. Factors associated with glomerular hyperfiltration in the early stage of hypertension. Am. J. Hypertens. 2012; 25:1011–1016. http://dx.doi.org/10.1038/ajh.2012.73. [PubMed: 22673015]

Peppa M, Brem H, Cai W, Zhang JG, Basgen J, Li Z, Vlassara H, Uribarri J. Prevention and reversal of diabetic nephropathy in db/db mice treated with alagebrium (ALT-711). Am. J. Nephrol. 2006; 26:430–436. [PubMed: 16974073]

Reeves W, Caulfield JP, Farquhar MG. Differentiation of epithelial foot processes and filtration slits: sequential appearance of occluding junctions, epithelial polyanion, and slit membranes in developing glomeruli. Lab. Invest. 1978; 39:90–100. [PubMed: 682603]

Reiter LW, Anderson GE, Laskey JW, Cahill DF. Developmental and behavioral changes in the rat during chronic exposure to lead. Environ. Health Perspect. 1975; 12:119–123. [PubMed: 1227852]

Schreuder M. Safety in glomerular numbers. Pediatr. Nephrol. 2012; 27:1881–1887. [PubMed: 22532329]

Seyer-Hansen K, Hansen J, Gundersen HJ. Renal hypertrophy in experimental diabetes. A morphometric study. Diabetologia. 1980; 18:501–505. [PubMed: 7418959]

Sobin C, Montoya MG, Parisi N, Schaub T, Cervantes M, Armijos RX. Microglial disruption in young mice with early chronic lead exposure. Toxicol. Lett. 2013; 15:00151–00153.

Sobin C, Parisi N, Schaub T, de la Riva E. A Bland–Altman comparison of the Lead Care(R) System and inductively coupled plasma mass spectrometry for detecting low-level lead in child whole blood samples. J. Med. Toxicol. 2011a; 7:24–32. http://dx.doi.org/10.1007/s13181-13010-10113-13187. [PubMed: 20886381]

Sobin C, Parisi N, Schaub T, Gutierrez M, Ortega AX. δ-Aminolevulinic acid dehydratase single nucleotide polymorphism 2 and peptide transporter 2*2 haplotype may differentially mediate lead exposure in male children. Arch. Environ. Contam. Toxicol. 2011b; 61(3):521–529. [PubMed: 21327641]

Spector J, Navas-Acien A, et al. Associations of blood lead with estimated glomerular filtration rate using MDRD, CKD-EPI and serum cystatin C-based equations. Nephrol. Dial. Transpl. 2011; 26:2786–2792.

Staessen J, Yeoman WB, Fletcher AE, Markowe HL, Marmot MG, Rose G, Semmence A, Shipley MJ, Bulpitt CJ. Blood lead concentration, renal function, and blood pressure in London civil servants. Br. J. Ind. Med. 1990; 47:442–447. [PubMed: 1974456]

Steenland K, Selevan S, Landrigan P. The mortality of lead smelter workers: an update. Am. J. Public Health. 1992; 82:1641–1644. [PubMed: 1456339]

Suzuki H, Tokuriki T, Saito K, Hishida A, Suzuki K. Glomerular hyper-filtration and hypertrophy in the rat hypoplastic kidney as a model of oligomeganephronic disease. Nephrol. Dial. Transplant. 2005; 20:1362–1369. [PubMed: 15870220]

Weibel, ER. Stereological Methods, Vol. 1, Practical Methods for Biological Morphometry. Academic Press; 1979.

Ziegler EE, Edwards BB, Jensen RL, Mahaffey KR, Fomon SJ. Absorption and retention of lead by infants. Pediatr. Res. 1978; 12:29–34. [PubMed: 643372]

Zuscik MJ, Ma L, Buckley T, Puzas JE, Drissi H, Schwarz EM, O'Keefe RJ. Lead induces chondrogenesis and alters transforming growth factor-beta and bone morphogenetic protein signaling in mesenchymal cell populations. Environ. Health Perspect. 2007; 115:1276–1282. [PubMed: 17805416]

HIGHLIGHTS

- Kidney structure was compared in young mice with and without chronic lead exposure.

- Mice with blood lead levels 2.4–4.7 μg/dl had increased glomerular volumes.

- Glomerular volume increase was the result of capillary and mesangial volume increases.

- Mice with blood lead levels 11.7–20.3 μg/dl did not have glomerular volume changes.
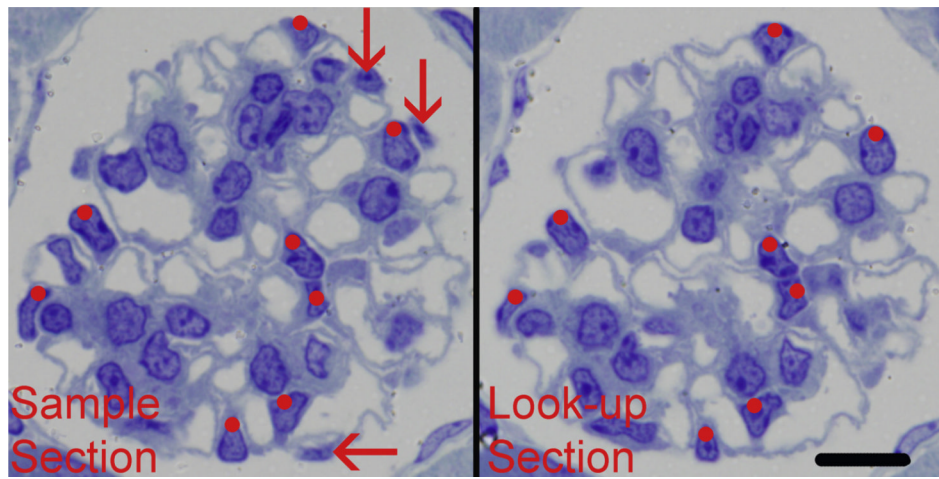
Fig. 1.
Disector sections used for counting podocytes. The two images from adjacent 1-mm thick sections formed a disector pair. Profiles from podocyte nuclei present in both sections were not counted (red dots). Profiles from podocyte nuclei present in the sample section but not present in the look-up section (red arrows) were counted as Q^-s and were used to calculate podocyte number. Scale bar = 10 µm.
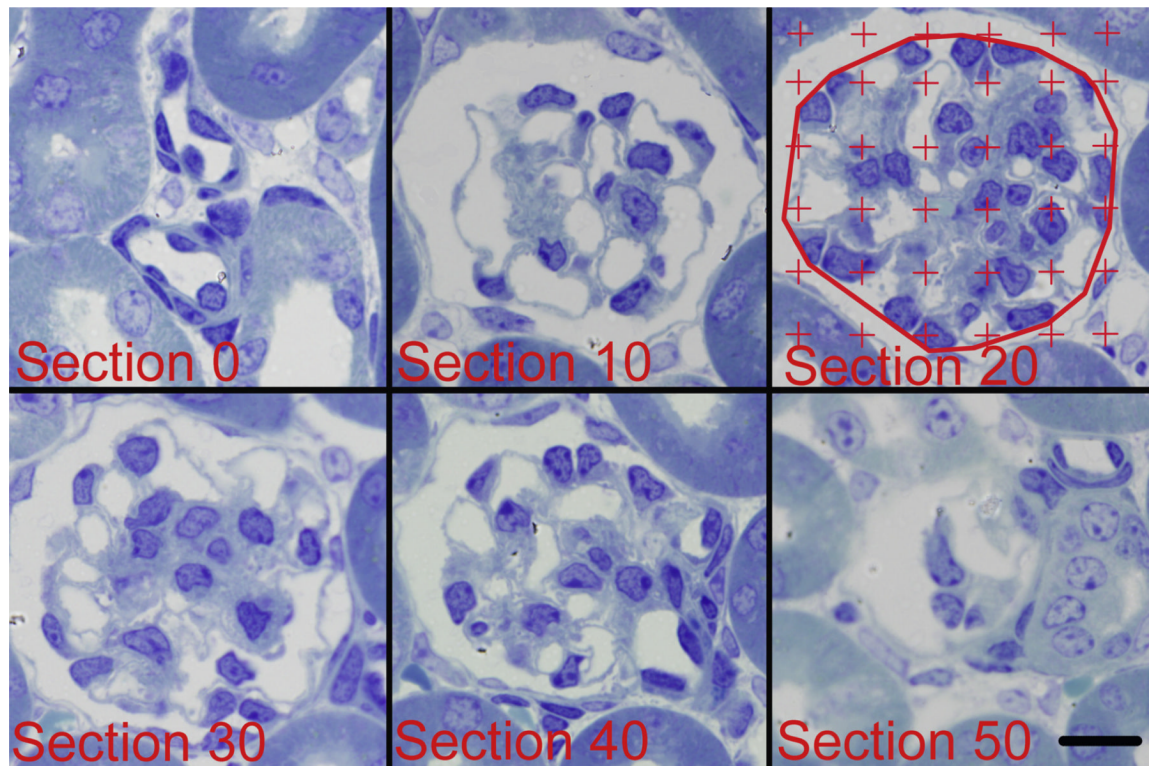
Fig. 2.
Six images (10 µm apart) from a glomerulus used to measure glomerular volume. The glomerulus was defined as the minimal string polygon surrounding the glomerular tuft as shown in Section 20. A counting grid was randomly placed over each image and the number of grid points falling on the glomerular profile was counted. Glomerular volume was calculated by multiplying the distance between sections (10 µm) by the sum of the points counted over all the glomerular profiles, and then multiplied by the area represented by 1 grid point. Scale bar = 10 µm.
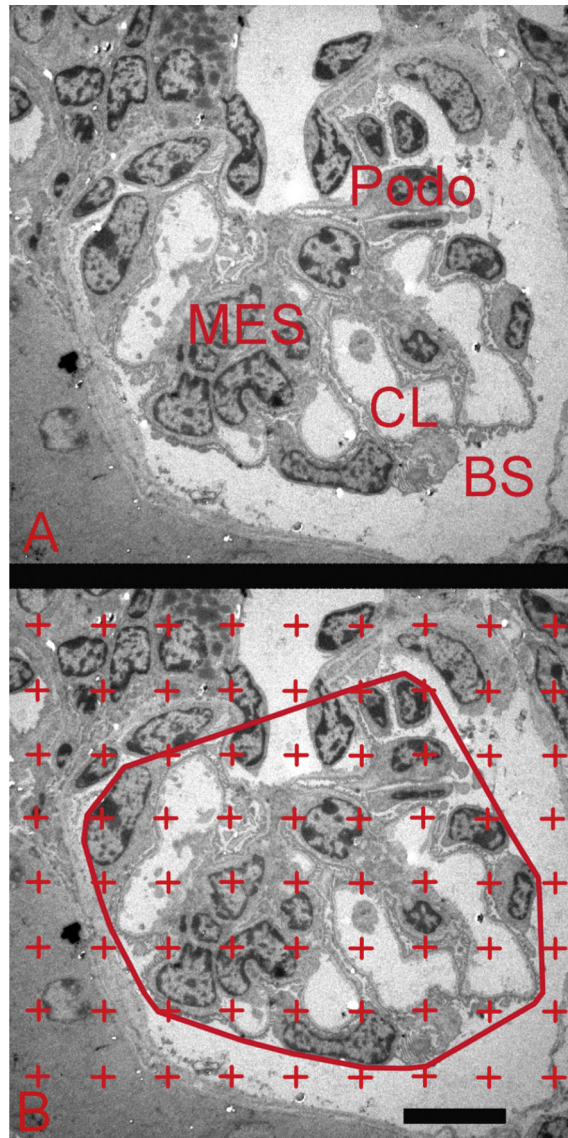
Fig. 3.
Electron microscopy image used to measure volume density of glomerular components. (A) Image of glomerular profile showing podocytes (Podo), mesangium (Mes), capillary lumen (CL), and Bowman's space (BM). (B) Image of a glomerular profile with counting grid. Glomerulus was defined as the minimal string polygon surrounding the glomerular tuft. The number of grid points falling on each of the four defined glomerular components was counted and used to calculate the volume density of each component. Scale bar = 10 μm.
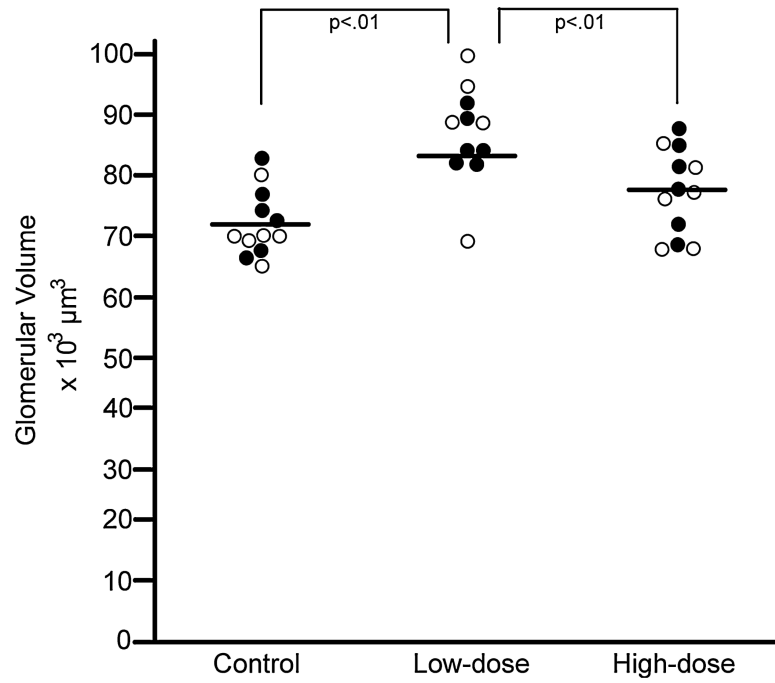
Fig. 4.
Glomerular volume. Graph shows individual mouse glomerular volume data at post-natal day 28 for the control, lose-dose, and high-dose groups. ● = male; ○ = female.

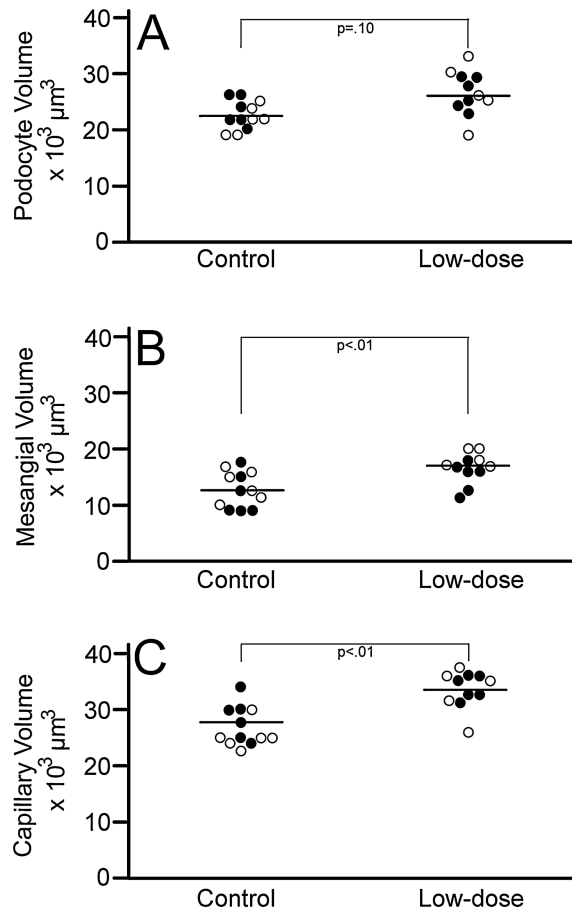**Fig. 5.**
Glomerular component volumes. Graph shows individual mouse data for podocyte volumes (Panel A), mesangial volumes (Panel B), and capillary volumes (Panel C) at post-natal day 28 for the control and lose-dose groups. ● = male; ○ = female.

Table 1

Mean (SD) of physiological characteristics of 28 day old C57BL6/J mice with and without lead exposure.

	Controls		Low-dose		High-dose	
	Males ($n = 6$)	Females ($n = 6$)	Males ($n = 6$)	Females ($n = 5$)	Males ($n = 6$)	Females ($n = 6$)
Blood lead level (μg/dL)[a]	0.03 (0.01)	0.03 (0.01)	3.63 (0.71)	2.74 (0.36)	16.02 (3.25)	13.35 (1.31)
Body weight (g)[b]	14.7 (1.3)	13.6 (1.3)	13.6 (0.6)	12.2 (1.2)	13.9 (1.5)	11.9 (1.5)
Kidney weight (mg)[b]	0.11 (0.01)	0.10 (0.02)	0.09 (0.01)	0.09 (0.01)	0.11 (0.01)	0.09 (0.02)

[a]ANOVA < 0.01.

[b]ANOVA < 0.05.

Table 2

Mean (SD) of podocyte number, glomerular volume and podocyte numerical density in young C57BL6/J mice with and without lead exposure (via light microscopy at 100×).

	Controls		Low-dose		High-dose	
	Males ($n = 6$)	Females ($n = 6$)	Males ($n = 6$)	Females ($n = 5$)	Males ($n = 6$)	Females ($n = 6$)
Podocyte number	70(9)	65(8)	70(7)	69(5)	67(3)	71(9)
Glomerular volume (μm^3)	73,513(6392)	70,916(4960)	85,744(4547)	88,051(11,312)	78,648(7367)	76,009(6902)
Podocyte numerical density ($\times 10^{-6}\,\mu m^{-3}$)	957(154)	925 (99)	828(69)	800(116)	862(61)	940(142)

Table 3

Mean (SD) of glomerular component volume density and volume in young C57BL/6J mice with and without lead exposure determined via electron microscopy at 3000×.

	Controls		Low-dose	
	Males (*n* = 6)	Females (*n* = 6)	Males (*n*=6)	Females (*n*=5)
Volume density				
Podocyte	0.319 (0.033)	0.314 (0.024)	0.307 (0.021)	0.301 (0.025)
Mesangium	0.165 (0.043)	0.196 (0.036)	0.177 (0.027)	0.212 (0.021)
Capillary lumen[a]	0.388 (0.031)	0.365 (0.008)	0.398 (0.016)	0.378 (0.016)
Remainder[b]	0.128 (0.024)	0.125 (0.027)	0.122 (0.019)	0.108 (0.012)
Volume				
Podocyte (μm^3)	23,416 (2473)	22,311 (2640)	26,306 (2440)	26,650 (5309)
Mesangium (μm^3)	12,173 (3608)	13,882 (2783)	15,154 (2417)	18,496 (1561)
Capillary lumen[a] (μm^3)	28,632 (3923)	25,802 (2056)	34,134 (1819)	33,208 (4650)
Remainder[b] (μm^3)	9419(1811)	8844 (1821)	10,427 (1702)	9395 (783)

[a]Including endothelial and circulating cells.

[b]Including Bowman's space, glomerular basement membrane, and non-resolvable tissue.